

Design and simulation of a caprylic acid enzymatically modified phosphatidylcholine micelle using a coarse-grained molecular dynamics simulations approach

Dalia Santos-Luna, Yudibeth Sixto-López, Diego Bravo-Alfaro, Cynthia Cano-Sarmiento, Hugo García & José Correa-Basurto

To cite this article: Dalia Santos-Luna, Yudibeth Sixto-López, Diego Bravo-Alfaro, Cynthia Cano-Sarmiento, Hugo García & José Correa-Basurto (2023): Design and simulation of a caprylic acid enzymatically modified phosphatidylcholine micelle using a coarse-grained molecular dynamics simulations approach, Journal of Biomolecular Structure and Dynamics, DOI: [10.1080/07391102.2023.2180434](https://doi.org/10.1080/07391102.2023.2180434)

To link to this article: <https://doi.org/10.1080/07391102.2023.2180434>



View supplementary material [↗](#)



Published online: 24 Feb 2023.



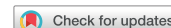
Submit your article to this journal [↗](#)



View related articles [↗](#)



View Crossmark data [↗](#)



Design and simulation of a caprylic acid enzymatically modified phosphatidylcholine micelle using a coarse-grained molecular dynamics simulations approach

Dalia Santos-Luna^{a*} , Yudibeth Sixto-López^{b,c*} , Diego Bravo-Alfaro^a , Cynthia Cano-Sarmiento^d , Hugo García^a  and José Correa-Basurto^c 

^aUnidad de Investigación y Desarrollo de Alimentos, Tecnológico Nacional de México/IT de Veracruz, Veracruz, México; ^bDepartamento de Química Farmacéutica y Orgánica, Facultad de Farmacia, Universidad de Granada, Campus de Cartuja, Granada, Spain; ^cLaboratorio de Diseño y Desarrollo de Nuevos Fármacos e Innovación Biotecnológica (Laboratory for the Design and Development of New Drugs and Biotechnological Innovation) SEPI-ESM, Instituto Politécnico Nacional, México, Mexico City, Mexico; ^dCONACyT-Unidad de Investigación y Desarrollo de Alimentos, Tecnológico Nacional de México/IT de Veracruz, Veracruz, México

Communicated by Ramaswamy H. Sarma

ABSTRACT

Computationally simulated micelle models provide useful structural information on the molecular and biological sciences. One strategy to study the self-aggregation process of surfactant molecules that make up a micelle is through molecular dynamics (MD) simulations. In this study, a theoretical approach with a coarse-grained MD simulation (CG-MD) was employed to evaluate the critical micellar concentration (CMC), the micellization process, building a tridimensional (3D) model system of a micelle using data from the experimentally enzymatically modified phospholipids (PL) by phospholipase A1 (PLA1). This required enzymatic interesterification of soybean phosphatidylcholine (PC) with caprylic acid, along with purification and characterization by chromatographic techniques to measure the esterified fatty acids and the corresponding PL composition. The number of molecules used in the CG-MD simulation system was determined from the experimental CMC data which was 0.025%. The molecular composition of the system is: **1** C 18:2, **2** C 8:0/8:0, **3** C 8:0/18:3n-9, **4** C 8:0/18:0, **5** C 8:0/18:2n-6, **6** C 8:0/18:1n-9, and **7** C 8:0/16:0. According to our theoretical results, the micelle model is structurally stable with an average R_g of $3.64 \pm 0.10 \text{ \AA}$, and might have an elliptical form with a radius of 24.6 \AA . Regarding CMC value there was a relationship between the experimental data of the modified PLs and the theoretical analysis by GC-MD, which suggest that the enzymatic modification of PLs does not affect their self-aggregation properties. Finally, the micellar system obtained in the current research can be used as a simple and useful model to design optimal biocompatible nanoemulsions as possible vehicles for bioactive small molecules.

ARTICLE HISTORY

Received 1 October 2022
Accepted 8 February 2023



KEYWORDS


Phospholipid; amphiphilic; interesterification; self-assembly; coarse grain

1. Introduction

Phospholipids (PL) are amphipathic molecules with wide applications in food, cosmetic and pharmaceutical industries as surfactants, dispersants, and humectants, among others (Lordan et al., 2017; Manikandan et al., 2019; McClements & Gumus, 2016; Singh et al., 2017). Because of their amphiphilic nature, the most important characteristic of PL is their ability to accumulate at the interface between two phases and reduce surface tension to form micelles. Micelles are basic structures useful to prepare model systems intended to study cell interactions, drug delivery, encapsulation of foods and bioactive compounds, among others. They can be used to encapsulate hydrophilic, hydrophobic and/or amphipathic compounds, increasing their bioavailability, in the case of

being used as carriers of active compounds to avoid physical or chemical degradation of the encapsulated compounds. During the formulation process the micelle structure must be optimized considering several factors. One of these is the type of PL employed, since each type of PL shows different physicochemical properties, their effect on the micelle stability is also specific and justifies being studied. The physicochemical properties of PLs depend on their molecular structure. PL can be modified chemically or enzymatically to change their native properties and prepare structured PL (Hudiyanti et al., 2014; Lin et al., 2017; Zhang et al., 2019). Phospholipase A1 (PLA 1) and phospholipase A2 (PLA 2) are two main classes of enzymes widely employed in enzymatic modifications of PL. These types of enzymatic reactions are regioselective and are carried out under near-environmental

CONTACT José Correa-Basurto ✉ jcorreab@ipn.mx; corrjose@gmail.com  Laboratorio de Diseño y Desarrollo de Nuevos Fármacos e Innovación Biotecnológica (Laboratory for the Design and Development of New Drugs and Biotechnological Innovation) SEPI-ESM, Instituto Politécnico Nacional, México, Plan de San Luis y Díaz Mirón S/N, Col. Casco de Santo Tomas, Mexico City, 11340, Mexico; Hugo García ✉ hugo.gg@veracruz.tecnm.mx  Unidad de Investigación y Desarrollo de Alimentos, Tecnológico Nacional de México/IT de Veracruz, M.A. de Quevedo 2779, Col. Formando Hogar, Veracruz, 91897, México.

 Supplemental data for this article can be accessed online at <https://doi.org/10.1080/07391102.2023.2180434>.

*These authors contributed equally.

conditions, preserving the original properties of heat- or oxygen-sensitive PL (Acevedo-Estupiñan et al., 2019; Ochoa-Flores et al., 2017). Structured PL are the product of this modification, which involves rearrangements of fatty acid residues (intraesterification), and acyl additions (esterification) or exchange (interesterification) at the sn-1 or sn-2 positions of the glycerol backbone (Ang et al., 2019; Gazolu.Rusanova et al., 2020; Verdasco-Martin et al., 2019). Soybean phosphatidylcholine (PC) is composed of saturated fatty acids, such as stearic or palmitic acid at the sn-1 position, while the sn-2 position is usually occupied by unsaturated fatty acids, i.e., oleic, linoleic, and arachidonic acids (Cao et al., 2012; Niezgodą & Gliszczynska, 2019; Tai et al., 2018). Current studies on PL structural modifications are mainly performed to guarantee their oxidative stability, incorporating health beneficial fatty acids, and in the case of micelle synthesis helps to improve their physicochemical stability, system permeability, and to increase the bioavailability of the transported compounds (Baeza-Jimenez et al., 2012; 2012; 2014; Chávez-Zamudio et al., 2017; García et al., 2008; Kim et al., 2010; Ochoa-Flores et al., 2013; Verdasco-Martin et al., 2019; Zhao et al., 2014).

Several experimental, theoretical, and computational studies have been performed on the PL self-assembly revealing that this process is highly dependent on the interactions between the dispersed phase and the dispersant phase (Allen & Lorenz, 2015; Brocos et al., 2012; Koshiyama et al., 2019). Aqueous PL solutions exhibit different aggregation states, forming more than one type of micellar structure, for example, spherical ovoid, and rod-shaped conformations (Chng, 2013; Faramarzi et al., 2017; Lebecque et al., 2017). If the chemical composition of PL changes, the structures resulting from their self-assembly will also change, as well as the long-term stability of the micelle (Hashemzadeh et al., 2020).

Molecular Dynamic (MD) simulation is a molecular modeling tool used to study molecular dynamic behavior. It can be employed to study at molecular level the lipid aggregation mechanisms and the stability of the aggregates formed along the time (Chatzidaki et al., 2017; Kamrani & Hadizadeh, 2019; Sanders & Panagiotopoulos, 2010). Currently, there are MD simulation methods that allow the study of the behavior of lipids in aqueous media at different media, capable of reproducing their physicochemical properties, at spatial and temporal scales, such as Coarse-Grained Molecular Dynamics (CG-MD). The use of MD simulations allows to reduce costs and experimental time and provides information on the structural behavior of the molecules studied over time in an aqueous environment, different types of systems can be studied including nanostructured systems, such as nanotubes or graphene-based nanomaterials and its participation in the development of diseases or in the case of micelle systems its assistance in drug delivery (Alimohammadi et al., 2020; Ehsan et al., 2021; Reza & Mohammad, 2021). CG-MD simplifies the electronic structure by forming systems of groups of atoms that are empirically parameterized. MARTINI is the CG-MD simulation force field most widely utilized (Hossain et al., 2019; Trujillo & Schramm, 2010). In this study, soybean PC

enzymatically modified with caprylic acid was used to form a micellar system; additionally, a CG-MD simulation approach was run to study the assembly and stability of the PL micelle system.

2. Materials and methods

2.1. Materials

Phospholipase PLA1 (Lecitase Ultra®) was kindly donated by Novozymes (Barcelona, Spain), while Duolite A568 was a gift from Rohm and Haas (Barcelona, Spain). Lecithin (PC, 95% phosphatidylcholine), was purchased from Avanti Polar Lipids, Inc. (Alabaster, AL). Caprylic acid was obtained from SIGMA-ALDRICH (Mexico City). HPLC grade solvents were purchased from Tecsiquim (Mexico City) and all other reagents used were analytical grade from SIGMA-ALDRICH (Mexico City).

2.2. Phospholipid modification

2.2.1. Immobilization of PLA1

PLA1 was immobilized on an anion exchange resin with a particle size of 0.15-0.85 mm, by adsorption, following a previously described method (García et al., 2008): 10 g of PLA1 enzyme was mixed with 10 mL of 0.1 N Tris-HCl buffer (pH 8); this solution was put in contact with 2 g of support (Duolite A568). The mixture was placed on an orbital shaker at 300 rpm and 50 °C for 12 h. Immobilized enzyme was rinsed with 50 mL of buffer and dried at 30 °C, as it dried the support was used for the acidolysis reactions.

2.2.2. Acidolysis reaction catalyzed by immobilized PLA1

Modification of PC was carried out by acidolysis with minor modifications (Ochoa-Flores et al., 2017). A mixture of PC and caprylic acid was prepared in a molar ratio of 1:8; 4 mL of n-hexane was added to this solution for each gram of PC used. Finally, 10% of the total weight of the immobilized PLA1 substrates was used. The reaction was carried out for 24 h at 50 °C and 300 rpm on a MaxQ orbital shaker (Thermo Fisher Scientific, Waltham, MA). Aliquots were taken, periodically, to monitor the percentage of incorporation.

2.2.3. Gas chromatographic (GC) analysis of the percentage of caprylic acid incorporation

The percentage of caprylic acid incorporation was monitored following the methodology of Cavazos Gaduño et al. (Cavazos-Garduño et al., 2015), with minor modifications. An aliquot of 50 µL of the reaction mixture was taken and methylated with 2.5 mL of 0.5 M sodium methoxide for 10 min at 80 °C. Subsequently, 2 mL of n-hexane and 5 mL of a sodium carbonate solution (9 g NaCO₃ in 100 mL deionized water) were added. This solution was centrifuged at 3000 rpm for 10 min. The n-hexane phase was then recovered in GC vials. About 1 µL of the methylated sample was injected into a gas chromatograph (Hewlett-Packard model 6890) equipped with an HP-INNOWax capillary column (60 m

× 0.25 mm × 0.25 mm film thickness) and a flame ionization detector (FID), using the conditions described in a previous publication (Cavazos-Garduño et al., 2015). To perform peak identification, the retention times of the samples were compared with the analytical standard FAME Mix C4-C24 (SUPELCO, Bellefonte, PA). Esterified fatty acids were quantified using methyl tridecanoate (C13:0, 0.25 mg/mL) as an internal standard.

2.2.4. Performance analysis of the modified PC acidolysis reaction by HPLC

Quantification of the modified PC (PCm) during the acidolysis reaction was made using a Waters HPLC system equipped with a UV-Visible detector (Waters 2487), fitted with a normal phase silica column (5 µm, 250 × 4.6 mm, Econosil Silica, Alltech Associates, Inc.). The mobile phase was composed by isocratic ACN/MeOH/H₃PO₄ (130:5:1.5), at a flow rate of 1 mL/min, the UV detector was set at 205 nm. PC standard solutions were employed to prepare the calibration curve.

2.2.5. PCm purification by column chromatography

Open column chromatography was used to remove free fatty acids from the reaction mixture after acidolysis. The glass chromatographic column (55 × 560 mm) was packed by gravity with silica gel (60–200 mesh, 60 Å of mean pore diameter, Sigma Aldrich). A 1/100 weight ratio of product/silica gel was used. Chloroform (100%) was employed as a mobile phase for free fatty acids separation, and methanol (100%) for PL disaggregation. Fractionation was monitored by thin-layer chromatography (TLC), using aluminum backed silica chromatographic plates (20 × 20 cm, F-254, Dynamic Adsorbents®). Phosphomolybdic acid in methanol (10%) was used as a TLC developing agent, and plates were heated on a heating plate.

2.3. Determination of the critical micellar concentration of the PCm

The critical micellar concentration (CMC) of PCm was determined from the change in the slope of the surface tension values versus surfactant concentration, according to Trujillo and Schramm (Pires et al., 2012). This method directly determines the actual equilibrium surface tension values. Surface tension of the modified PC solutions was measured using the Wilhelmy's plate method, using a DataPhysics DCAT₁₁ tensiometer, and for control, analysis and measurement of the test, the SCAT 31 software was employed. Each one of the solutions were prepared fresh at the time of the analysis with deionized water, at 17 ± 1 °C; surfactant concentrations were expressed as a percentage of dissolved solids. The platinum plate surface was first washed with deionized water, acetone, and red-hot burned under flame to completely remove adsorbed surfactants.

2.4. General procedure for coarse-grain molecular dynamics

The Gromacs software package version 5.1.4 (DeLano, 2002) was used to perform all MD simulations. Using the Martini force field (version 2.2), the conditions for MD were analyzed, such as: dynamics time, temperature, pressure, box size and then phospholipid, and water molecules were added, respectively. Then, as a first step, an energy minimization was performed to obtain a micellar pre-structure. The objective of performing this minimization is to eliminate interactions, which do not fit or are not required between the phospholipid molecules and thus to have as a result the proper interactions between the phospholipid molecules and the solvent molecules. In this way, the simulation system will get the lowest energy. The number of steps for the energy minimization stage was 3000 steps. At equilibrium, the system pressure was considered constant (1 bar), and the system temperature was set to 298 K by V-rescale method and Berendsen barostat method. After performing system minimization, equilibration was achieved, the time step was 30 fs, with an isothermal-isothermal-isobaric (NPT) assembly to relax the micelle structure and the simulation time was 150 ns (ACD/ChemSketch, 2019; Brocos et al., 2012; Faramarzi et al., 2017; Hashemzadeh et al., 2020; National Center for Biotechnology Information, 2018; Trujillo & Schramm, 2010). The times for the molecular dynamics simulations performed in this work were 300 ns and for 1000 ns. The trajectory analysis was performed using the GROMACS package tools and the PyMOL™ 2.3.2 software (Marrink et al., 2007).

2.4.1. Lipid topologies

Parameterization of structurally modified phospholipid molecules was performed. The construction of the molecules was based on a randomization of the fatty acids obtained in the chromatographic profile. To create these molecules, reference topologies, reported in the chemical database PubChem, there were used to generate atomistic data, then each molecule was minimized using the ACD/ChemSketch 14.51 software (National Center for Biotechnology Information, 2018), to extract the parameters to the coarse-grain model. The PL molecules used as a basis were the following: DPPC (C18:0), DFPC (C18:3), DTPC (C8:0), DOPC (C18:1(9C)), DLPC (C12:0), IPC (C18:2), and DIPPC (C18:2, 9c,12c) (Marrink et al., 2004; Yang et al., 2005) (Supplement material).

MARTINI topologies and lipid coordinate files available in the MARTINI lipidome database (Li et al., 2010), were needed to adapt the molecular topology; itp (atoms, bonds, and angles), and gro? of the structures, by file mapping to confirm that the virtual chemical modifications of the files were appropriate, PyMOL2.3.2 software was used to render the molecular images. Both were necessary to start the simulation process in the GROMACS environment (Li et al., 2010). The MARTINI force field uses a 4:1 mapping scheme for non-ring structures, where on average 4 heavy atoms are represented by 1 interaction center (Trujillo & Schramm, 2010).

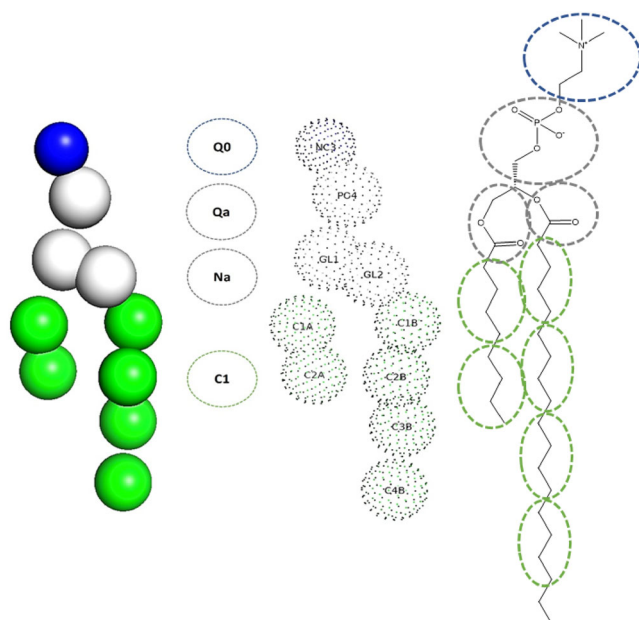


Figure 1. CG model for DPPC. PLs used in MD simulations include NC3 (navy blue), PO4, GL1 and GL2 (white), C1A, C1B, C3A, C2A, C2B, C3B, and C4B (green) beads.

In the CG representation, the PL head consists of two hydrophilic groups: the choline (Q0 type) and the phosphate group (Qa) (Figure 1). Two intermediate hydrophilic sites (Na) to represent the glycerol ester. Lipid tails (C1), representing the fatty acids, and a central one (C4) representing the double bond, the number of beads depending on the fatty acid, either in the *sn*-1 and *sn*-2 positions of the PL. Non-bonded interactions between directly unconnected particles were excluded.

2.4.2. CG molecular dynamics simulations

To confirm the analysis corresponding to the CMC study, and to analyze the self-assembly of the PLs. The simulation was based on a random distribution of molecules in a 13 nm cube-shaped box. In total, 100 PL molecules were added in the box. The number of components was based on a randomization of the fatty acids that conform the molecules of PLs, taking into consideration the profile of fatty acids obtained by GC, and in the theoretical composition of the fatty acids located at positions *sn*-1 and *sn*-2 of the PL (Cao et al., 2012; Tai et al., 2018). The system composition was as follows: 37 molecules of DPPC, 18 of DFPC, 15 of DTPC, 11 of DOPC, 10 of DLPC, 7 of IPC, and 2 of DIPC, in 16,452 CG water beads. The energy minimization steps were equal to 3000 steps and constant volume equilibrium to adjust the temperature to 298 K and constant pressure equilibrium to adjust the pressure at 1 bar.

3. Results and discussion

3.1. Enzymatic modification of phosphatidylcholine

In this study, the highest PLA1 incorporation (98%) in Duolite A568 was achieved after 8 h at 50 °C. These results

are consistent with the data of Cavazos-Garduño et al. (Cavazos-Garduño et al., 2015). The purpose of immobilizing the enzyme is to increase the inter-esterification of fatty acids and to be able to reuse the enzyme without affecting its activity (Baeza-Jimenez et al., 2012; Kim et al., 2010; Ochoa-Flores et al., 2013). Once the PLA1 was immobilized on the support, the initial PC was modified by replacing the long-chain fatty acids with caprylic acid. The determination of the % incorporation of caprylic acid into the initial PC was determined by derivatization with alkaline methylation using 0.5 N sodium methoxide and subsequent analysis by gas chromatography.

Figure 2 shows the comparative profile of the fatty acids of the initial PC and the PCm, when carrying out the quantification of the fatty acids by % mole of the initial PC and the PCm as shown in Table 1. The outcome was the incorporation of caprylic acid into the PC, with a C8:0 esterification of $57.44 \pm 1.24\%$. In our previous report the incorporation of C8:0 was smaller than the one achieved in this work (42.32%) (Ochoa-Flores et al., 2017). Figure 3 shows the kinetics of the fatty acid incorporation as a function of time in % mol. Our higher PLA1 incorporation may be attributed to the use of organic solvents during the reaction, producing a migration of acyls, upon interesterification, causing an intra-esterification of fatty acids from the *sn*-1 to *sn*-2 position of the PL (Egger et al., 1997; Silva et al., 2012). This phenomenon may explain the increase in the molar incorporation of C8:0 with respect to other studies (ACD/ChemSketch, 2019; Acevedo-Estupiñan et al., 2019; Alimohammadi et al., 2020; Allen & Lorenz, 2015; Ang et al., 2019; Baeza-Jimenez et al., 2012; 2012; 2014; Brocos et al., 2012; Cao et al., 2012; Cavazos-Garduño et al., 2015; Chatzidaki et al., 2017; Chávez-Zamudio et al., 2017; Chng, 2013; DeLano, 2002; Ehsan et al., 2021; Faramarzi et al., 2017; García et al., 2008; Gazolu.Rusanova et al., 2020; Hashemzadeh et al., 2020; Hossain et al., 2019; Kamrani & Hadizadeh, 2019; Kim et al., 2010; Koshiyama et al., 2019; Lebecque et al., 2017; Marrink et al., 2004; 2007; National Center for Biotechnology Information, 2018; Niezgoda & Gliszczynska, 2019; Ochoa-Flores et al., 2013; 2017; Pires et al., 2012; Reza & Mohammad, 2021; Sanders & Panagiotopoulos, 2010; Tai et al., 2018; Trujillo & Schramm, 2010; Verdasco-Martin et al., 2019; Zhao et al., 2014).

The HPLC analysis showed a yield of $46.4 \pm 3.04\%$ (wt%) of the PC which was successfully modified by PLA1; the percentage of the remaining reaction corresponded to lysophosphatidylcholine, unmodified PC and free fatty acids. The chromatograms obtained from time zero and 24 h of the reaction are shown in Figure 4. In a related work (Ochoa-Flores et al., 2017) our group reached a conversion of PC to PCm of 53.02%, this is due to the fact that, in comparison with the present work, the presence of water molecules in acidolysis, promotes the intra-esterification of fatty acids, producing lysophosphatidylcholine, and thus diminish the yield of PCm. Figure 5 depicts the kinetics of the incorporation of caprylic acid, the yield of PC and PCm (Acevedo-Estupiñan et al., 2019; Ang et al., 2019; Ochoa-Flores et al., 2017).

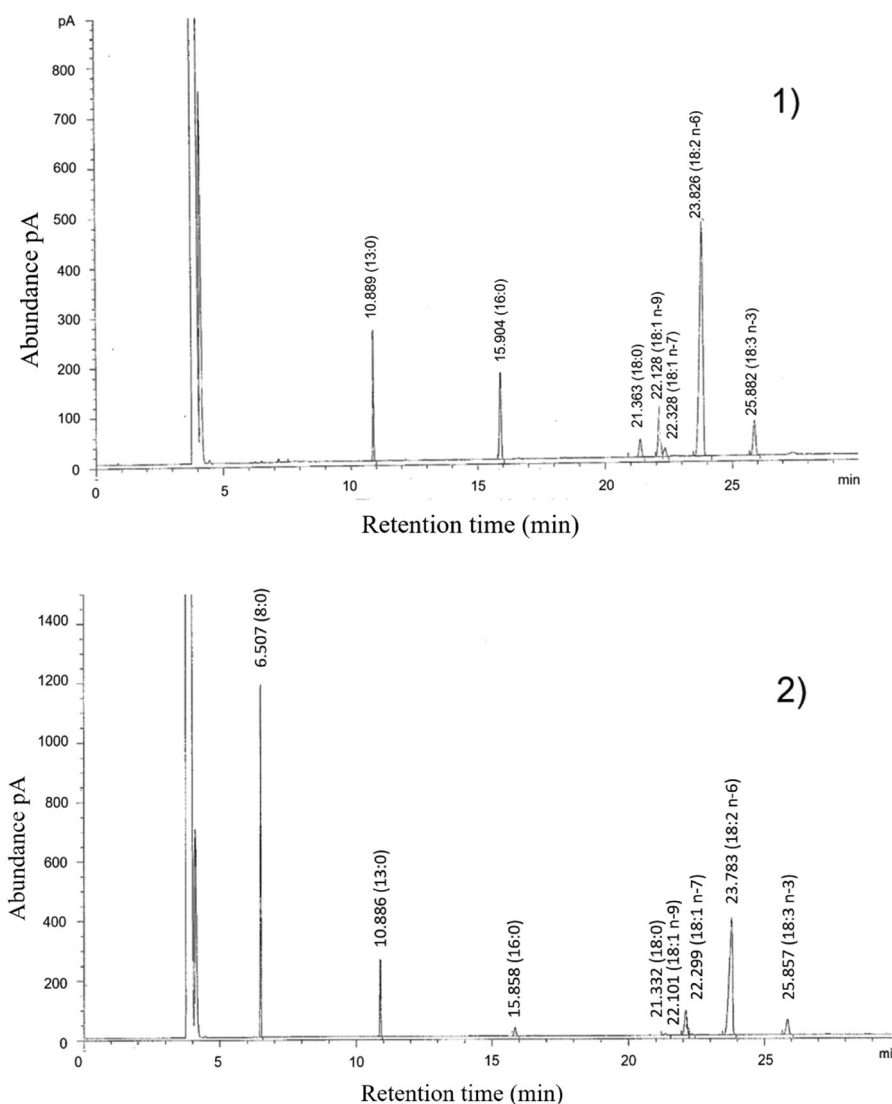


Figure 2. Fatty acid composition profile of (a) initial PC and (b) MPC, detected by gas chromatography. Experimental conditions: 1 μ L was used for injection, 190 $^{\circ}$ C initial temperature and a ramp of 4 $^{\circ}$ C per minute until 210 $^{\circ}$ C was reached. The run times were 30 min.

Table 1. Comparison of the fatty acid profile of native and modified phosphatidylcholine.

Fatty acid	PC	PCm
C8:0	—	57.44 \pm 1.07
C16:0	14.90 \pm 0.05	5.43 \pm 0.12
C18:0	3.70 \pm 0.03	1.51 \pm 0.05
C18:1	11.40 \pm 0.02	4.99 \pm 0.09
C18:2	63.00 \pm 0.02	27.61 \pm 0.83
C18:3	5.70 \pm 0.08	3.02 \pm 0.04

The reaction decreased with increasing concentration of free fatty acids (Egger et al., 1997). This is a consequence of increased viscosity, low water solubility or polarity changes in the reaction medium. However, the degree of conversion depends on the chain length and the degree of instability of the fatty acid to be incorporated into the PL molecule; caprylic acid, a medium-chain saturated fatty acid, being the fatty acid favored as a substrate by PLA1 (Egger et al., 1997).

The entries correspond to the mean \pm SD ($n = 3$)

3.2. Critical micellar concentration of the PCm

Surface tension of a surfactant-containing solution changes abruptly when the CMC is exceeded (Patist et al., 2000). This is caused by the solution properties which depend on whether the surfactant molecules are dispersed as monomers or aggregated as micelles (Sou et al., 2000). CMC values decrease with increasing hydrophilicity of lipid molecules with longer hydrocarbon chains. Our results are consistent with the literature, by increasing the hydrophilicity of the phospholipid, being an amphiphilic molecule, CMC increased (Ashok et al., 2004; Patist et al., 2000; Sou et al., 2000). In the case of PCm, the structural modification made mainly at the sn-1 position of PL, when adding a medium-chain fatty acid, influenced the CMC. The CMC of our system was found at 0.025% concentration of surfactant, as shown in the graph of surface tension vs PCm concentration (Figure 6), where the two lines intersect. The PCm surface tension concentration graphs show two straight lines with different slopes. The intersection of these

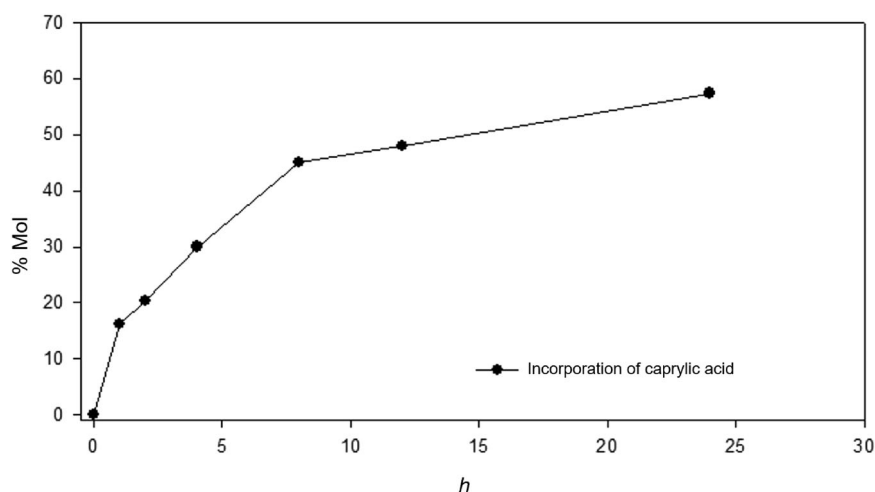


Figure 3. Kinetics of MCFA incorporation into PC by the enzyme phospholipase A1. Reaction conditions: 10% w/w of immobilized enzyme with respect to the substrate mixture, with orbital shaking at 300 rpm for 24 h.

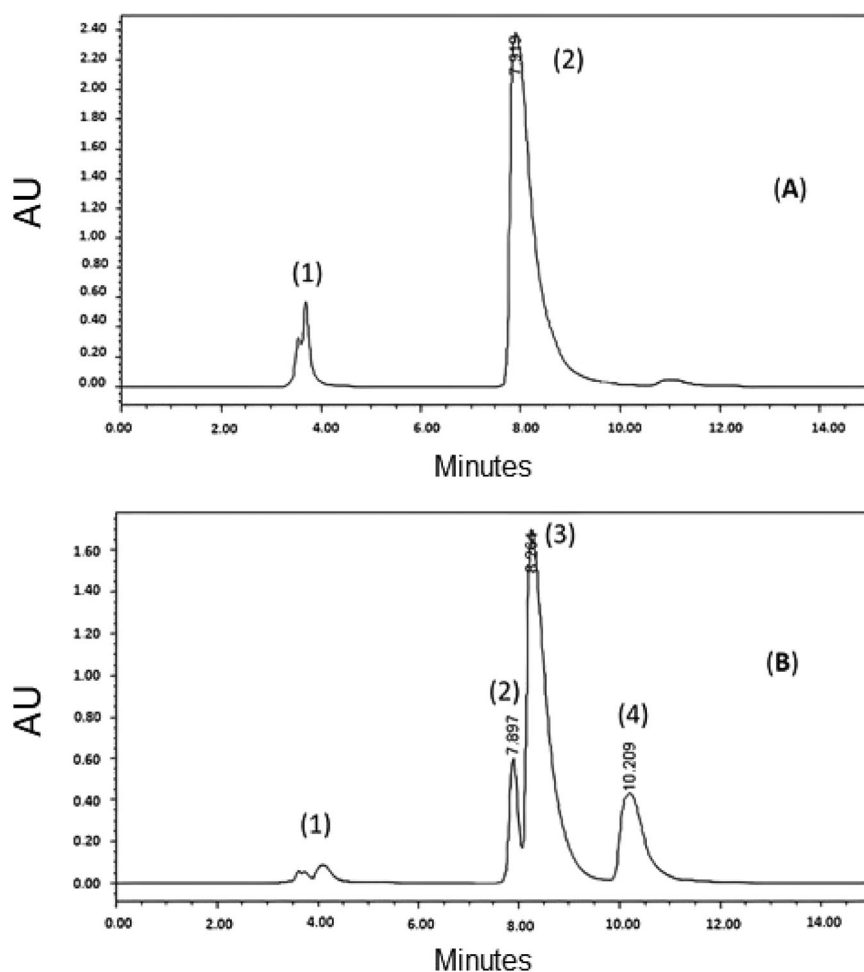


Figure 4. Chromatograms obtained by HPLC of the hydrolysis reaction products for the conversion of PC to MPC. (A) zero reaction time where the peak (1) corresponds to FA, (2) to PC, and (B) at 24 h of reaction, where the peak (1) corresponds to FA, (2) PC, (3) PCm, and (4) LPC.

two straight lines gives the CMC value of PCm. Concentrations below the CMC indicate dispersed monomers in the solution, as the surfactant concentration increases, the interfacial tension on the surface decreases, caused by the aggregation of monomers on the surface of the solution (Sou et al., 2000).

3.3. Molecular structures that make up the PCm

Assembly of the phospholipid molecules, which resulted from the randomization of the fatty acids, from the fatty acid profile obtained by gas chromatography (Table 1) was: **1** C 18:2, **2** C 8:0/8:0, **3** C 8:0/18:3n-9, **4** C 8:0/18:0, **5** C 8:0/18:2n-6, **6** C 8:0/18:1n-9, and **7** C 8:0/16:0. These results were

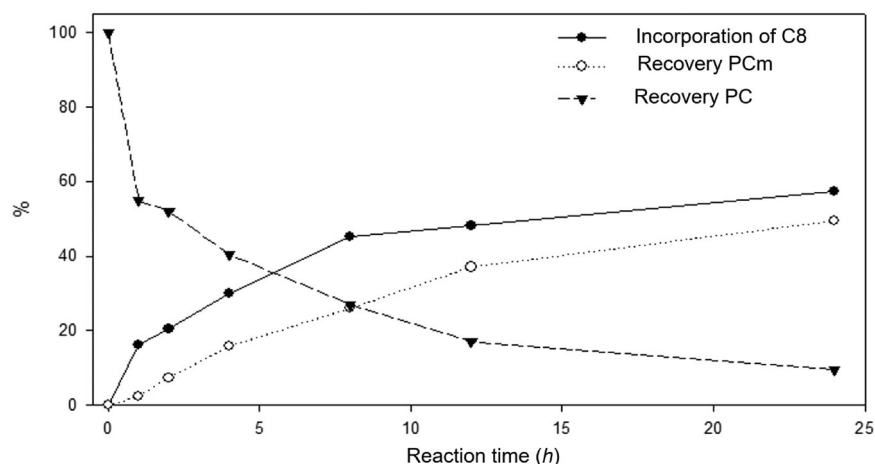


Figure 5. Kinetics of molar incorporation of medium cadmium fatty acids and molar concentration of PC and MPC in the acidolysis reaction catalyzed by phospholipase A1. Reaction conditions: 10% w/w of immobilized enzyme with respect to the substrate mixture, with orbital shaking at 300 rpm for 24 h.

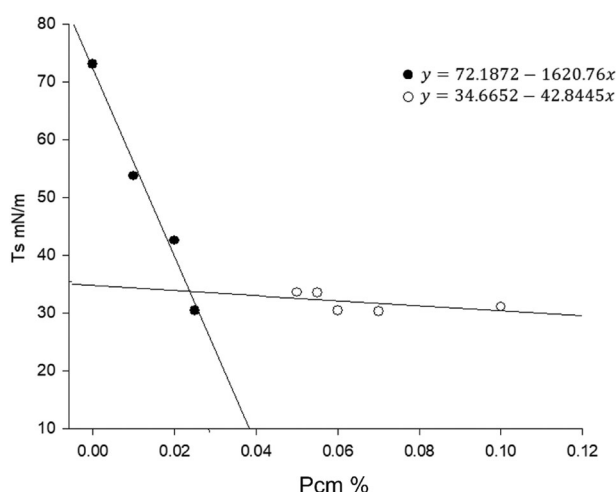


Figure 6. Change in surface tension versus surfactant concentration, for the determination of the surface tension of PCm CMC at $T = 17 \pm 1^\circ\text{C}$.

considered to determine the number of molecules that build up the micelle submitted to CG-MD simulation, which represents the CMC at 0.025%.

3.4. Self-assembly of PCm molecules

In this work, we assayed the use of enzymatically modified phospholipid molecules to provide the self-assembly process and create a micellar structure model using MD simulation fed by our experimental micelle results. To build the micellar system, we performed two types of CG-MD simulation. The first simulation was 300 ns, and the goal was to allow the randomly placed PLs to self-assemble to form the micelle. At the beginning of this simulation small aggregates started to form. PL given their amphipathic character as their concentration in an aqueous medium increase, they tend to self-assemble (DeLano, 2002). The self-assembly of the phospholipids gives rise in the early stages of the dynamics to molecular aggregates of different sizes, which are formed by PLs with similar hydrocarbon chains (Figure 7A). Some authors (Israelachvili, 2011; Koshiyama et al., 2019; Sangwai & Sureshkumar, 2011; Tieleman et al., 2000) suggest that the

hydrophobicity of the system controls the formation of micelles, creating a rotation of the structure, attracting the hydrocarbon tails to each other, while the head groups tend to align themselves exposed to water. These results suggest that the enzymatic modification performed on PC did not affect its physicochemical characteristics, resulting in a meta-stable system. An increase in monomer aggregates is observed, this persists along the 300 ns-long of MD simulation time and accompanied by the formation and breakage of PCm micelles, the assembled phospholipid groups grew by collision and formed nanodiscs and bowl-shaped patches. The process of self-assembly was visualized in these dynamics, during which the components of the system, such as the modified PL, were in a disordered state at the beginning of the MD, and as time progressed an ordered structure was formed (Figure 7A,B). The PL created a lipid polymorphism in the early stages of dynamics, possibly caused by the composition of the hydrocarbon chain of the fatty acid that forms the PL, intermolecular interactions, temperature, and pressure. These factors play an important role in the formation of stable systems such as nanoemulsions.

The phospholipid aggregates then coalesced due to random motion and fluctuation to form an elliptical closed micelle, which evolved to an oval form (Figure 7C). These results are related to those reported by Koshiyama et al. (Rui & Dias, 2007) where, the formation of vesicles, in three phases is observed, i.e., the formation of bicelles, bowls and a micellar structure. Intermolecular forces play an important role for the self-assembly of PLs, depending on their structural conformation, the shape of the final micellar structure.

Once the micelle was assembled, the stability of the system was assayed in a second CG-MD simulation of 1000 ns-long. Therefore, the second MD simulation was fed with pre-assembled micelle (Figure 7D-F). As expected, the closed and oval form of the micelle was maintained, with free monomers in the dispersion phase. It is worth noting that the temperature of this simulation was the same as the experimental one, which allows inferring that the experimental conditions led to the formation of a stable micelle system which can be further used to encapsule and transport different substances, including drugs.

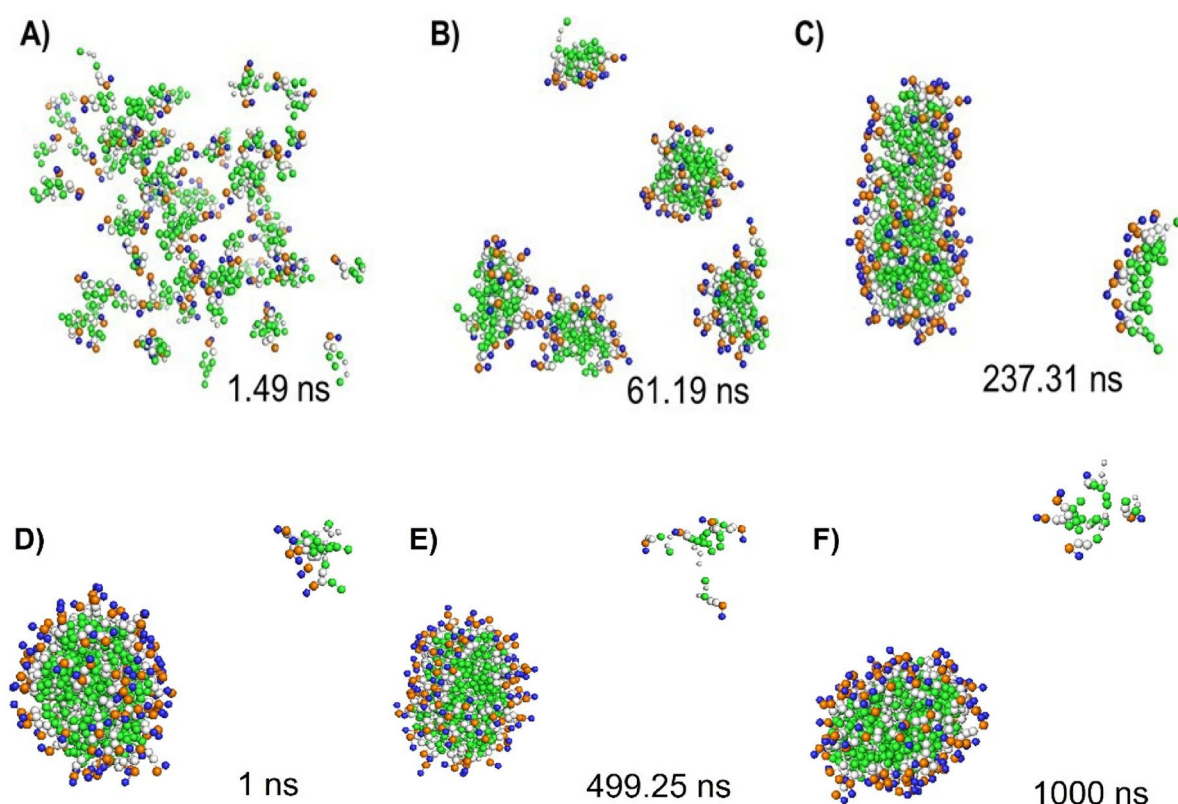


Figure 7. Formation and stability of the micelles observed during the CG-MD simulations. Snapshots of the spontaneous aggregation process at a PCm concentration of 0.025% PL. In snapshots (A), (B), and (C), the micelle system was preassembled with a 300 ns-long MD simulation. The micelle increases in size with collision and assembly of the phospholipid bundles, until finally a micelle is formed. The stability of the Micelle was observed in our 1000 ns-long CG-MD simulation (D), (E), and (F). The PLs are represented as beads, the carbon atoms are colored green, the phosphate groups orange, the choline blue and the glycerol portion white.

3.5. Micelle structural details

3.5.1. Stability of the system

As mentioned above a 300 ns-long MD simulation was carried out to assemble the system and test if the experimental CMC led to the formation of a micellar system. To investigate the transition dynamics of PL aggregation, Figure 8 shows the variation of the radius of gyration (Rg) of the micelle as a function of time. The equilibrium of the systems was monitored through the Rg, as well as by visual inspection. A detriment in Rg suggests self-assembly of phospholipid molecules to aggregate (Figures 7A–C and 8A), followed by compaction into a micelle Figure 7(D). The Rg indicates the compactness of the system and through it the assembly of phospholipid molecules can be inferred, as the value of Rg decreases, the micellar structure is formed (Kiessling et al., 2006), as depicted in Figure 8(A). At the beginning of the simulation, the PLs were dispersed (Figure 7A,B), as the simulation time elapsed, the self-assembly was unified (Figures 8A and 7A–C). Therefore, at the end of the 300 ns-simulation, the PL molecules had the lowest value of the Rg Figure 8(A).

Figure 8(A) shows the Rg in the self-assembly process of the micelle (300 ns-simulation), where the Rg was significantly reduced as expected. Whereas that during the 1000 ns-simulation in Figure 8(B) the stability of the Rg was observed. Even when at the beginning the micelle shows a little increment but from 50 ns the Rg was stable, suggesting that the micelle obtained under our experimental conditions is stable and can be further used. PL can freely rotate along

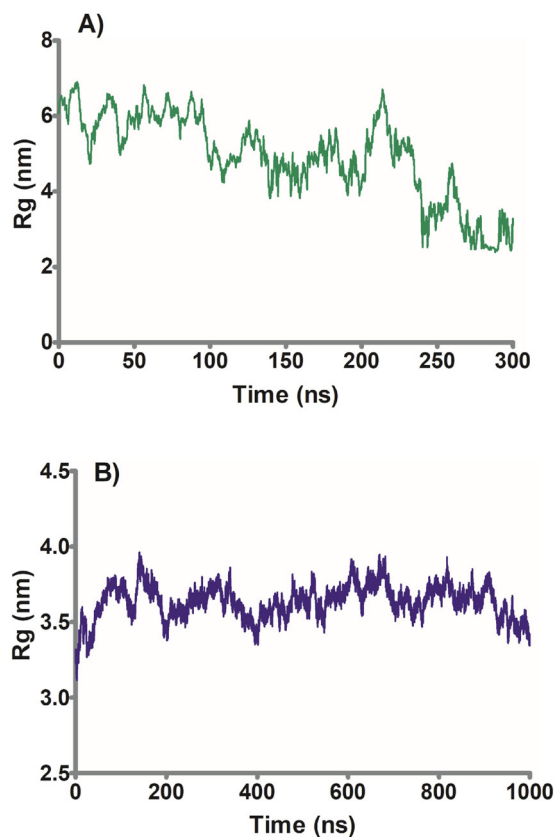


Figure 8. Rg of the PL's as a function of simulation time (ps). (A) Rg of the pre-assembly. (B) Rg of the assembled micelle.

their longitudinal axis; their fatty acid tails can flex and diffuse laterally. Because of this mobility, micelles are fluid. In fact, when lateral diffusion is so fast, a PL can diffuse laterally within the micelle from one end to the other (Gupta et al., 2018; Levi & Gratton, 2007).

Further, the lateral diffusion of the PL was favored because of the rotation and translational motions induce by the interaction between them and with the water of the system due to repulsive non-bond interaction which induce a rapid and random movements generated to form the micelle, to this end the mean square displacement (MSD) was calculated (Figure 9). The MSD calculation is based on the Einstein relation. In the MSD plot, the slope of the curve increases with time, the displacement is random and can be considered as Brownian motion (Fujiwara et al., 2002; Stadler et al., 2012).

Once the closed micellar model structure was formed there was an increment of MSD. Figure 10 indicates the MSD parameter on the time scale of 1000 ns. From the micellar model, conformed by modified PLs, a significant MSD was obtained, due to the interactions between the particles (rotations, movement, and intermolecular vibrational modes), increasing the interactions between the hydrophobic heads of the PLs decreased their movements (Lange et al., 2020). Figure 10 shows the increase of the MSD parameter as the

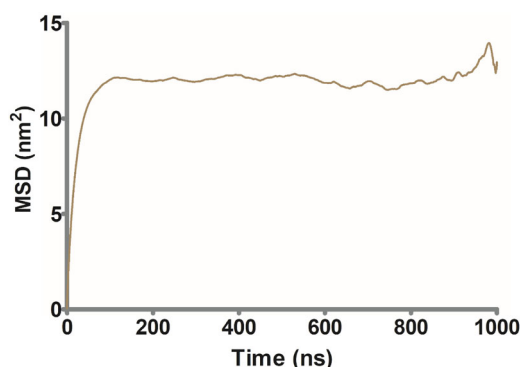


Figure 9. The MSD (mean square displacement) of PL's of the formed micelle.

micelle is generated, this parameter is plotted according to the MD time, when the final micelle is generated, the maximum value is reached. One of the advantages of the model made in this work is that the micelle generated is stable over time and can be a suitable candidate for the delivery of bioactive compounds.

3.5.2. Micelle shape

From the assembled micelle, the shape of the micelle was characterized. First, the sphericity was determined by the eccentricity of the micelle, which is defined as:

$$e = 1 - I_{\min}/I_{\text{avg}} \quad (1)$$

where, I_{\min} is the minimum components of the moment of inertia along the principal axes of the inertia tensor; that is, x , y , or z axis, and I_{avg} is the average of the three principal axes of the moment of inertia (Palazzesi et al., 2011). Following the above formula (1), the eccentricity is 0.691 ± 0.019 (Figure 10A), which suggests that the micelle takes an elliptical form as observed in the final snapshot of 1000 ns (Figure 10B). A micelle with a spherical form takes an eccentricity value of 0.

The effective radius of our micelle is 24.6 \AA . The mean radius of the micelle R_s is defined as:

$$R_s = \sqrt{\frac{5}{3} R_g} \quad (2)$$

where, R_g is the average of the radius of gyration (Palazzesi et al., 2011) from the stable zone of the MD simulation, which was $3.64 \pm 0.10 \text{ \AA}$, from 53 to 1000 ns.

4. Conclusions

Micellar models have applications in different biotechnological areas, one of them being biomedicine. The encapsulation of bioactive compounds, increasing their stability and bioavailability. Furthermore, the main objective is to generate 3D models from experimental data to be studied under MD simulations to explore their molecular structure properties. In

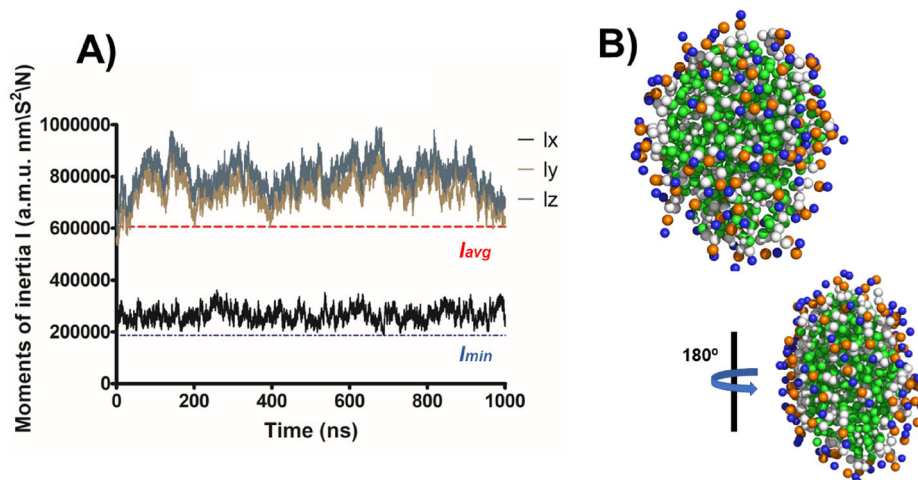


Figure 10. Eccentricity of the micelle in 1000 ns long CG-MD simulation. (A) The moment of inertia during the simulation of the axes x , y , and z are depicted as black, brown, and blue lines, respectively. The average of the inertia is pointed out with dotted red line and the minimum of inertia with blue dotted line. (B) 1000 ns representative snapshots of the micellar system are depicted, where from two different angles can be observed that the micelle adopts an elliptic form.

this work, soybean PC were enzymatically modified by phospholipase A1 using caprylic acid, which were further characterized and used for performing a micellar system. The obtained CMC of the micelle was 0.025% concentration of surfactant. According to GC the molecular composition of the system is: **1** C 18:2, **2** C 8:0/8:0, **3** C 8:0/18:3n-9, **4** C 8:0/18:0, **5** C8:0/18:2n-6, **6** C8:0/18:1n-9, and **7** C 8:0/16:0. The experimental results were used to model a micelle using CG-MD simulation. According to CG-MD simulation results (average R_g 3.64 ± 0.10 Å), the micelle model is structurally stable and might have an elliptical form with a radius of 24.6 Å.

Finally, we propose that the simulated micellar structure could be useful to better understand the self-assembly of PLs, moreover, it is suitable in the design of nanostructured systems as transporters of bioactive compounds.

Acknowledgment

Y.S.L. thanks to SECTEI (Secretaría de Educación, Ciencia, Tecnología e Innovación de la Ciudad de México) for a Postdoctoral Fellowship.

Disclosure statement

The authors have no relevant financial or non-financial interests to disclose.

Funding

This work was supported by 250784 and CB-254600 granted by The National Council for Science and Technology of Mexico (CONACyT). The authors gratefully acknowledge the scholarship from CONACyT for graduate studies of authors Santos-Luna D., and Bravo-Alfaro D.A.

ORCID

Dalia Santos-Luna  <http://orcid.org/0000-0002-4757-1519>
Yudibeth Sixto-López  <http://orcid.org/0000-0001-8903-3834>
Diego Bravo-Alfaro  <http://orcid.org/0000-0003-3612-7743>
Cynthia Cano-Sarmiento  <http://orcid.org/0000-0002-9079-6748>
Hugo García  <http://orcid.org/0000-0001-5805-0201>
José Correa-Basurto  <http://orcid.org/0000-0002-4973-5265>

Author's contribution

D.S.L. and Y. S. L., wrote the manuscript, made the figures, and analyzed theoretical results; D.S.L. D. B. A., and C. C. S. performed experimental assays; D.S.L., Y. S. L., H. S. G., and J. C. B. designed the project and wrote the manuscript. All authors read and approved the final manuscript.

References

- ACD/ChemSketch. (2019). Version 2019.14.51, Advanced Chemistry Development, Inc., Toronto, ON, Canada, www.acdlabs.com.
- Acevedo-Estupiñan, M. V., Gutierrez-Lopez, G. F., Cano-Sarmiento, C., Parra-Escudero, C. O., Rodriguez-Estrada, M. T., García-Varela, R., & García, H. S. (2019). Stability and characterization of O/W free phytosterols nanoemulsions formulated with an enzymatically modified emulsifier. *LWT- Food Science and Technology*, 107, 151–157. <https://doi.org/10.1016/j.lwt.2019.03.004>
- Alimohammadi, E., Khedri, M., Miri Jahromi, A., Maleki, R., & Rezaian, M. (2020). Graphene-based nanoparticles as potential treatment options for parkinson's disease: a molecular dynamics study. *International Journal of Nanomedicine*, 15, 6887–6903. <https://doi.org/10.2147/IJN.S265140>
- Allen, D. T., & Lorenz, C. D. (2015). Molecular scale simulations of the self-assembly of amphiphilic molecules: Current state-of-the-art and future directions. *Journal of Self-Assembly and Molecular Electronics*, 3, 1–38.
- Ang, X., Chen, H., Xiang, J. Q., Wei, F., & Quek, S. Y. (2019). Preparation and functionality of lipase-catalysed structured phospholipid: A review. *Trends in Food Science & Technology*, 88, 373–383. <https://doi.org/10.1016/j.tifs.2019.04.005>
- Ashok, B., Arleth, L., Hjelm, R. P., Rubinstein, I., & Önyüksel, H. (2004). In Vitro Characterization of PEGylated Phospholipid micelles for improver drug solubilization: Effect of PEG chain length and PC incorporation. *Journal of Pharmaceutical Sciences*, 93(10), 2476–2487. <https://doi.org/10.1002/jps.20150>
- Baeza-Jimenez, R., González-Rodríguez, J., Kim, I.-H., García, H. S., & Otero, C. (2012). Use of immobilized phospholipase A₁-catalyzed acidolysis for the production of structured phosphatidylcholine with an elevated conjugated linoleic acid content. *Grasas y Aceites*, 63(1), 44–52.
- Baeza-Jimenez, R., López-Martinez, L. X., & García, H. S. (2014). Biocatalytic modification of food lipids: Reactions and applications. *Revista Mexicana de Ingeniería Química*, 13(1), 29–47.
- Baeza-Jimenez, R., Noriega-Rodríguez, J. A., García, H. S., & Otero, C. (2012). Structured phosphatidylcholine with elevated content of conjugated linoleic acid: Optimization by response surface methodology. *European Journal of Lipid Science and Technology*, 114(11), 1261–1267. <https://doi.org/10.1002/ejlt.201200038>
- Brocos, P., Mendoza-Espinosa, P., Castillo, R., Mas-Oliva, J., & Piñeiro, Á. (2012). Multiscale molecular dynamics simulations of micelles: coarse-grain for self-assembly and atomic resolution for finer details. *Soft Matter*, 8(34), 9005. <https://doi.org/10.1039/c2sm25877c>
- Cao, W., Zhang, K., Tao, G., Wang, X., & Liu, Y. (2012). Identification of the fatty acyl residues composition and molecular species of phosphatidylcholines in soy lecithin powder by UPLC-ESI-MS/MS. *Cromatographia*, 75(21-22), 1271–1278. <https://doi.org/10.1007/s10337-012-2309-2>
- Cavazos-Garduño, A., Ochoa Flores, A. A., Serrano-Niño, J. C., Martínez-Sánchez, C. E., Beristain, C. I., & García, H. S. (2015). Preparation of betulinic acid nanoemulsions stabilized by omega-3 enriched phosphatidylcholine. *Ultrasonics Sonochemistry*, 24, 204–213. <https://doi.org/10.1016/j.ultsonch.2014.12.007>
- Chatzidakis, M. D., Papavasileiou, K. D., Papadopoulos, M. G., & Xenakis, A. (2017). Reverse micelles as antioxidant carriers: An experimental and molecular dynamics study. *Langmuir*, 22, 5077–5085.
- Chávez-Zamudio, R., Ochoa-Flores, A. A., Soto-Rodríguez, I., García-Varela, R., & García, H. S. (2017). Preparation, characterization and bioavailability by oral administration of O/W curcumin nanoemulsions stabilized with lysophosphatidylcholine. *Food & Function*, 8(9), 3346–3354. <https://doi.org/10.1039/C7FO00933J>
- Chng, C. P. (2013). Effect of simulation temperature on phospholipid bilayer-vesicle transition studied by coarse-grained molecular dynamics simulations. *Soft Matter*, 9(30), 7294–7301. <https://doi.org/10.1039/c3sm51038g>
- DeLano, W. L. (2002). PyMOL. DeLano Scientific.
- Egger, D., Wehtje, E., & Adlercreutz, P. (1997). Characterization and optimization of phospholipase A2 catalyzed synthesis of phosphatidylcholine. *Biochimica et Biophysica Acta*, 1343(1), 76–84.
- Ehsan, A., Arash, N., Mohammad, K., Milad, R., Ahnmad, M., Nima, R., & Reza, M. (2021). Potential treatment of Parkinson's disease using new-generation carbon nanotubes: a biomolecular *in silico* study. *Future Medicine*, 16(3)
- Faramarzi, S., Bonnett, B., Scaggs, C. A., Hoffmaster, A., Grodi, D., Harvey, E., & Mertz, B. (2017). Molecular dynamics simulations as a tool for accurate determination of surfactant micelle properties. *Langmuir : The ACS Journal of Surfaces and Colloids*, 33(38), 9934–9943. <https://doi.org/10.1021/acs.langmuir.7b02666>
- Fujiwara, T., Ritchie, K., Murakoshi, H., Jacob, K., & Kusumi, A. (2002). Phospholipids undergo hop diffusion in compartmentalized cell

- membrane. *The Journal of Cell Biology*, 157(6), 1071–1081. <https://doi.org/10.1083/jcb.200202050>
- García, H. S., Kim, I.-H., López-Hernandez, A., & Hill, C. G. Jr., (2008). Enrichment of lecithin with n-3 fatty acids by acidolysis using immobilized phospholipase A1. *Grasas y Aceites*, 59(4), 368–374. <https://doi.org/10.3989/gya.2008.v59.i4.531>
- Gazolu.Rusanova, D., Mustan, F., Vinarov, Z., Tcholakova, S., Denkov, N., Stoyanov, S., & Folter, J. W. (2020). Role of lysophospholipids on the interfacial and liquid film properties of enzymatically modified egg yolk solutions. *Food Hydrocolloids*, 99, 105319. <https://doi.org/10.1016/j.foodhyd.2019.105319>
- Gupta, S., De Mel, J. U., Perera, R. M., Zolnierczuk, P., Bleuel, M., Faraone, A., & Schneider, G. J. (2018). Dynamics of phospholipid membranes beyond thermal undulations. *The Journal of Physical Chemistry Letters*, 9(11), 2956–2960. <https://doi.org/10.1021/acs.jpclett.8b01008>
- Hashemzadeh, H., Javadi, H., & Darvishi, M. H. (2020). Study of structural stability and formation mechanisms in DSPC and DPSM liposomes: A coarse-grained molecular dynamics simulation. *Scientific Reports*, 10(1), 1837. <https://doi.org/10.1038/s41598-020-58730-z>
- Hossain, M. S., Berg, S., Bergström, C. A. S., & Larsson, P. (2019). Aggregation behavior of medium chain fatty acids studied by coarse-grained molecular dynamics simulation. *AAPS PharmSciTech*, 20(2), 61. <https://doi.org/10.1208/s12249-018-1289-4>
- Hudiyanti, D., Radifar, M., Raharjo, T. J., Narsito, N., & Noegrohati, S. (2014). A coarse-grained molecular dynamics simulation using NAMD package to reveal aggregation profile of phospholipids self-assembly in water. *Journal of Chemistry*, 6(2014)
- Israelachvili, J. N. (2011). *Intermolecular and surface forces* (3rd ed). Academic Press.
- Kamrani, S. M. E., & Hadizadeh, F. (2019). A coarse-grain MD (molecular dynamic) simulation of PCL-PEG and PLA-PEG aggregation as a computational model for prediction of the drug-loading efficacy of doxorubicin. *Journal of Biomolecular Structure and Dynamics*, 37(16), 4215–4221. <https://doi.org/10.1080/07391102.2018.1541762>
- Kiessling, V., Crane, J., & Tamm, L. (2006). Transbilayer. Effects of raft-like lipid domains in asymmetric planar bilayers measured by single molecule tracking. *Biophysical Journal*, 91(9), 3313–3326. <https://doi.org/10.1529/biophysj.106.091421>
- Kim, I.-H., García, H. S., & Hill, C. G. Jr., (2010). Synthesis of structured phosphatidylcholine containing n-3 PUFA residues via acidolysis mediated by immobilized phospholipase A₁. *Journal of the American Oil Chemists' Society*, 87(11), 1293–1299. <https://doi.org/10.1007/s11746-010-1609-7>
- Koshiyama, K., Taneo, M., Shigematsu, T., & Wada, S. (2019). Bicelle-to-vesicle transition of a binary phospholipid mixture guided by controlled local lipid compositions: A molecular dynamics simulation study. *The Journal of Physical Chemistry. B*, 123(14), 3118–3123. <https://doi.org/10.1021/acs.jpcb.8b10682>
- Lange, N., Leermakers, F. A. M., & Kleijn, J. M. (2020). Self-limiting aggregation of phospholipid vesicles. *Soft Matter*, 16(9), 2379–2389. <https://doi.org/10.1039/c9sm01692a>
- Lebecque, S., Crowet, J. M., Nasir, M. N., Deleu, M., & Lins, L. (2017). Molecular dynamics study of micelles properties according to their size. *Journal of Molecular Graphics and Modeling*, 72, 6–15. <https://doi.org/10.1016/j.jmgm.2016.12.007>
- Levi, V., & Gratton, E. (2007). Exploring dynamics in living cells by tracking single particles. *Cell Biochemistry and Biophysics*, 48(1), 1–15. <https://doi.org/10.1007/s12013-007-0010-0>
- Li, W., Du, W., Li, Q., Sun, T., & Liu, D. (2010). Study on acyl migration kinetics of partial glycerides: Dependence on temperature and water activity. *Journal of Molecular Catalysis B: Enzymatic*, 63(1–2), 17–22. <https://doi.org/10.1016/j.molcatb.2009.11.012>
- Li, W., Li, R. W., Li, Q., Du, W., & Liu, D. (2010). Acyl migration and kinetics study of 1(3)-positional specific lipase of *Rhizopus oryzae*-catalyzed methanolysis of triglyceride for biodiesel production. *Process Biochemistry*, 45(12), 1888–1893. <https://doi.org/10.1016/j.procbio.2010.03.034>
- Lin, M. H., Hung, C. F., Aljuffali, I. A., Sung, C. T., Huang, C. T., & Fang, J. Y. (2017). Cationic amphiphile in phospholipid bilayer or oil–water interface of nanocarriers affects planktonic and biofilm bacteria killing. *Nanomedicine : nanotechnology, Biology, and Medicine*, 13(2), 353–361. <https://doi.org/10.1016/j.nano.2016.08.011>
- Lordan, R., Tsoupras, A., & Zabetakis, I. (2017). Phospholipids of animal and marine origin: Structure, function, and anti-inflammatory properties. *Molecules*, 22(11), 1964. <https://doi.org/10.3390/molecules22111964>
- Manikandan, A., Divakar, D., & Poonam, S. N. (2019). Phospholipid-the dynamic structure between living and non-living world; a much obligatory supramolecule for present and future. *AIMS Molecular Science*, 6(1), 1–19.
- Marrink, S. J., de Vries, A. H., & Mark, A. E. (2004). Coarse grained model for semi-quantitative lipid simulations. *The Journal of Physical Chemistry B*, 108(2), 750–760. <https://doi.org/10.1021/jp036508g>
- Marrink, S. J., Risselada, H. J., Yefimov, S., Tieleman, P. D., & Vries, A. H. (2007). The MARTINI force field: Coarse grained model for biomolecular simulations. *The Journal of Physical Chemistry B*, 111(27), 7812–7824. <https://doi.org/10.1021/jp071097f>
- McClements, D. J., & Gumus, C. E. (2016). Natural emulsifier-biosurfactants, phospholipids, biopolymers, and colloidal particles: Molecular and physicochemical basis of functional performance. *Advances in Colloid and Interface Science*, 234, 3–26. <https://doi.org/10.1016/j.cis.2016.03.002>
- National Center for Biotechnology Information. (2018). PubChem substance record for SID 162093584, Source: ChEMBASE.cn. Retrieved September 25, from <https://pubchem.ncbi.nlm.nih.gov/substance/162093584>.
- Niezgoda, N., & Gliszczyńska, A. (2019). Lipase catalyzed acidolysis for efficient synthesis of phospholipids enriched with isomerically pure cis-9, trans-11 and trans-10, cis-12 conjugated linoleic acid. *Catalyst*, 9(12), 1012. <https://doi.org/10.3390/catal9121012>
- Ochoa-Flores, A. A., Hernández-Becerra, J. A., Cavazos-Garduño, A., Vernon-Carter, E. J., & García, H. S. (2017). Optimization of the synthesis of structured phosphatidylcholine with medium chain fatty acid. *Journal of Oleo Science*, 66(11), 1207–1215. <https://doi.org/10.5650/jos.ess17087>
- Ochoa-Flores, A. A., Hernández-Becerra, J. A., Cavazos-Garduño, A., García, H. S., & Vernon-Carter, E. J. (2013). Phosphatidylcholine enrichment with medium chain fatty acids by immobilized phospholipase A₁-catalyzed acidolysis. *Biotechnology Progress*, 29, 1.
- Palazzesi, F., Calvaresi, M., & Zerbetto, F. (2011). A molecular dynamics investigation of structure and dynamics of SDS and SDBS micelles. *Soft Matter*, 7(19), 9148. <https://doi.org/10.1039/c1sm05708a>
- Patist, A., Bhagwat, S. S., Penfield, K. W., Aikens, P., & Shah, D. O. (2000). On the Measurement of critical micelle concentrations of pure and technical-grade nonionic surfactants. *Journal of Surfactants and Detergents*, 3(1), 53–58. <https://doi.org/10.1007/s11743-000-0113-4>
- Pires, J. M., Moura, A. F. D., & Freitas, L. C. G. (2012). Investigating the spontaneous formation of sds micelle in aqueous solution using a coarse-grained force field. *Química Nova*, 35(5), 978–981. <https://doi.org/10.1590/S0100-40422012000500021>
- Reza, M., & Mohammad, A. (2021). Simultaneous doxorubicin encapsulation and in-situ microfluidic micellization of bio-targeted polymeric nanohybrids using dichalcogenide monolayers: A molecular in-silico study. *Materials Today Communications*, 26, 101948.
- Rui, M. C., & Dias, R. (2007). Prediction of mean square radius of gyration of tree-like polymers by a general kinetic approach. *Polymers*, 1785–1801.
- Sanders, S. A., & Panagiotopoulos, A. Z. (2010). Micellization behavior of coarse-grained surfactant model. *The Journal of Chemical Physics*, 132(11), 114902. <https://doi.org/10.1063/1.3358354>
- Sangwai, A. V., & Sureshkumar, R. (2011). Coarse-grained molecular dynamics simulations of the sphere to rod transition in surfactant micelles. *Langmuir : The ACS Journal of Surfaces and Colloids*, 27(11), 6628–6638. <https://doi.org/10.1021/la2006315>
- Silva, R. C., Soares, F., Hazzan, M., Capacla, R. I., Goncalves, A. M., & Gioielli, L. A. (2012). Continuous enzymatic interesterification of lard and soybean oil blend: Effects of different flow rates on physical properties and acyl migration. *Journal of Molecular Catalysis B: Enzymatic*, 23–28.

- Singh, R. P., Gangadharappa, H. V., & Mruthunjaya, K. (2017). Phospholipids: Unique carriers for drug delivery systems. *Journal of Drug Delivery Science and Technology*, 39, 166–179. <https://doi.org/10.1016/j.jddst.2017.03.027>
- Sou, K., Endo, T., Takeoka, S., & Tsuchida, E. (2000). Poly (ethylene glycol)-modification of the phospholipid vesicle by using the spontaneous incorporation of poly (ethylene glycol)- lipid into the vesicle. *Bioconjugate Chemistry*, 11(3), 372–379. <https://doi.org/10.1021/bc990135y>
- Stadler, A. M., Garvey, C. J., Bocahut, A., Sacquin-Mora, S., Digel, I., Schneider, G. J., Natali, F., Artmann, G. M., & Zaccai, G. (2012). Thermal fluctuations of haemoglobin from different species: adaptation to temperature via conformational dynamics. *Journal of the Royal Society Interface*, 9(76), 2845–2855. <https://doi.org/10.1098/rsif.2012.0364>
- Tai, K., Liu, F., He, X., Ma, P., Mao, L., Gao, Y., & Yuan, F. (2018). The effect of sterol derivatives on properties of soybean and egg yolk lecithin liposomes: Stability, structure and membrane characteristics. *Food Research International*, 109, 24–34. <https://doi.org/10.1016/j.foodres.2018.04.014>
- Tieleman, D. P., Spoel, D. V., & Berendsen, J. C. (2000). Molecular dynamics simulations of dodecylphosphocholine micelles at three different Aggregate Sizes: Micellar structure and chain relaxation. *The Journal of Physical Chemistry B*, 104(27), 6380–6388. <https://doi.org/10.1021/jp001268f>
- Trujillo, M., & Schramm, M. P. (2010). Measuring critical micelle concentration as a function of cavitand additives using surface tension and dye micellization. *Ronald E McNair Postbaccalaureate Achievement Program*, 14, 155–168.
- Verdasco-Martin, C. M., Corchado-Lopo, C., Fernández-Lafuente, R., & Otero, C. (2019). Rapid and high yield production of phospholipids enriched in CLA via acidolysis: The critical role of the enzyme immobilization protocol. *Food Chemistry*, 296, 123–131. <https://doi.org/10.1016/j.foodchem.2019.05.107>
- Yang, T., Fruekilde, M. B., & Xu, X. (2005). Suppression of acyl migration in enzymatic production of structured lipids through temperature programming. *Food Chemistry*, 92(1), 101–107. <https://doi.org/10.1016/j.foodchem.2004.07.007>
- Zhang, J., Yang, S., Cai, W., Yin, F., Jia, J., Zhou, D., & Zhu, B. (2019). Efficient production of medium-chain structured phospholipids over mesoporous organosulfonic acid-functionalized SBA-15 catalysts. *Catalyst*, 9(9), 770. <https://doi.org/10.3390/catal9090770>
- Zhao, T., No, D. S., Kim, B. H., García, H. S., Kim, Y., & Kim, I.-H. (2014). Immobilized phospholipase A1-catalyzed modification of phosphatidylcholine with $n-3$ polyunsaturated fatty acid. *Food Chemistry*, 157, 132–140. <https://doi.org/10.1016/j.foodchem.2014.02.024>